Wave packet dynamics in a two-dimensional electron gas with spin orbit coupling: Splitting and *zitterbewegung*

V. Ya. Demikhovskii, G. M. Maksimova, and E. V. Frolova*
Nizhny Novgorod State University, Gagarin Avenue, 23, Nizhny Novgorod 603950, Russian Federation
(Received 30 May 2008; published 3 September 2008)

We study the effect of splitting and *Zitterbewegung* of one- and two-dimensional electron wave packets in the semiconductor quantum well under the influence of the Rashba spin orbit coupling. Results of our investigations show that the spin orbit interaction induces dramatic qualitative changes in the evolution of spin-polarized wave packet. The initial wave packet with spin polarization splits into two parts, which propagate with unequal group velocity. This splitting appears due to the presence of two branches of electron spectrum corresponding to the stationary states with different chirality. It is also demonstrated that in the presence of external magnetic field **B** perpendicular to the electron-gas plane the wave packet splits into two parts, which rotate with different cyclotron frequencies. It was shown that after some periods, the electron density distributes around cyclotron orbit and the motion acquires an irregular character. Our calculations were made for both cases of weak and strong spin orbit couplings.

DOI: 10.1103/PhysRevB.78.115401 PACS number(s): 73.21.Hb, 71.10.Pm, 72.10.−d, 73.23.−b

I. INTRODUCTION

Producing and detecting spin-polarized currents in semiconductor nonmagnetic devices are the ultimate goals of spintronics. The intrinsic spin orbit interaction[1] existing in low-dimensional systems, which couples electron momentum to its spin, is one of the most promising tools for realizing spin-polarized transport. For these reasons, during the last years, a substantial amount of work has been devoted to study effects of spin orbit interaction on the transport properties of nanostructures (for a review, see, e. g., Refs. 2–4).

For the first time, the electron wave packet dynamics including the problem of *Zitterbewegung* in semiconductor quantum well under the influence of the spin orbit Rashba and Dresselhaus coupling has been considered by Schliemann *et al.*[5,6] In this work, the oscillatory motion of the electron wave packets reminiscent of the *Zitterbewegung* of relativistic electrons was studied for free-electron motion, i.e., in the absence of electric or magnetic fields. The authors of Refs. 5 and 6 predicted the resonance amplification of *Zitterbewegung* oscillations for the electron (moving in a quantum wire with parabolic confinement potential) and proposed to observe this fundamental phenomena, experimentally, using high-resolution scanning probe microscopy imaging techniques.

The *Zitterbewegung* of the heavy and light holes in three-dimensional (3D) semiconductors was investigated in Ref. 7. In this paper, the semiclassical motion of holes in the presence of a constant electric field was studied by numerical solution of the Heisenberg equations for momentum and spin operators in the Lattinger model of spectrum. It was shown that the hole semiclassical trajectories contain rapid small amplitude oscillations reminiscent of the *Zitterbewegung* of relativistic electrons. It should be noted, however, that the spatial structure of the wave packet and the changing of its shape due to effect of splitting in Refs. 8 and 9 was not considered.

At the same time, the splitting of spin-polarized electron beams in the systems with spin orbit coupling was investigated in a series of works. In particular, the authors of Refs. 8 and 9 propose to use the lateral interface between two regions in gated two-dimensional (2D) heterostructure with different strength of spin orbit coupling to polarize the electron. They have shown theoretically that in this structure, a beam with a nonzero angle of incidence splits into some spin-polarization components propagating at different angles. The similar effect of electron-spin-polarized reflection in heterostructures and spatial separation of the electron beams after reflection has been observed experimentally in Ref. 10.

The transverse electron focusing in systems with spin orbit coupling in the presence of perpendicular magnetic field was theoretically analyzed in Ref. 11, where it was shown that in the weak magnetic-field regime and for a given energy, the two branches of states have different cyclotron radii. The effect of spatial separation of the electron trajectories of different spin states, in a perpendicular magnetic field, has been experimentally observed in Ref. 12.

The authors of Refs. 13 and 14 considered the interplay between the spin orbit coupling and cyclotron motion in a perpendicular magnetic field, using the analogy between the Jaynes-Cumming model of atom transitions in a radiation field and the Rashba Hamiltonian in a perpendicular magnetic field.

In a recent paper by Schliemann,[15] the modifications of classical cyclotron orbits due to Rashba linear spin orbit coupling were explored. It was shown that the center of the wave packet moves on the more or less distorted spiral trajectories which forms depend on the initial spin orientation. So, the electron dynamics is not adequately described by semiclassical approximations. The numerical calculations of the expectation value of the packet coordinates $\bar{x}(t)$ and $\bar{y}(t)$ and packet width were made for the total time equals to five to six cyclotron periods.

In this work, we study the striking dynamics of the electron wave packets in a narrow A_3B_5 quantum well at the presence of the spin orbit k-linear Rashba coupling, which arises due to structural inversion ("up-down") asymmetry. The splitting of the wave packets in two parts appears due to

the presence of the electron states with "plus" and "minus" chiralities, which propagate with different group velocity. These two parts of the split packet can be characterized by different spin density. It is found that electron trajectories contain small amplitude damped oscillations. We show that the packet splitting leads to the damping of *Zitterbewegung*. The splitting and *Zitterbewegung* of wave packet is naturally accompanied by its broadening due to the effect of dispersion.

We also investigate the atypical cyclotron dynamics of the wave packet in a perpendicular magnetic field. It was shown that due to the spin orbit coupling, the packet with spin parallel to the magnetic field splits into two parts, which rotate with different cyclotron frequencies. We determine the moments when two parts of the packet are located at opposite points of the cyclotron orbit and, after that, they return (many times) back to their initial state. With the time due to the incommensurability of the cyclotron frequencies and the ordinary packet broadening, the electron density distributes randomly around the cyclotron orbit. All our calculations were made for the material parameters of the real semiconductor structures with a relatively strong and weak spin orbit and Zeeman interactions.

The paper is organized as follows. In Sec. II we introduce the Green's functions for 2D electrons in the presence of Rashba spin orbit interaction and analyze the evolution of one-dimensional (1D) wave packet. The analytical and numerical results illustrate the effects of packet splitting and *Zitterbewegung*. In Sec. III we describe in detail the time development of the 2D wave packets. Finally, in Sec. IV, we discuss the manifestation of the spin orbit interaction in the evolution of coherent wave packet in a magnetic field perpendicular to electron-gas plane. The splitting of the initial coherent packet and distribution electron probability via cyclotron orbit is considered. Section V concludes with a discussion of the results. The Appendix provides the mathematical details necessary to obtain Eqs. (36a) and (36b).

II. DYNAMIC OF THE ONE-DIMENSIONAL WAVE PACKETS

In this section we consider the specific character of the wave packet dynamics in the systems with Rashba spin orbit coupling.[1] The Hamiltonian of the system under consideration reads

$$H = H_0 + H_R = \frac{\mathbf{p}^2}{2m} + \alpha(\hat{p}_y\hat{\sigma}_x - \hat{p}_x\hat{\sigma}_y), \tag{1}$$

where $\mathbf{p}=-i\hbar\nabla$ is the momentum operator, m is the electron effective mass, α is the Rashba coupling constant, and the components of the vector σ denote the spin Pauli matrices. The eigenfunctions for the in-plane motion identified by the quantum numbers $\mathbf{p}(p_x,p_y)$ are

$$\phi_{\mathbf{p},s}(\mathbf{r}) = \frac{1}{2\sqrt{2}\pi\hbar} e^{i\mathbf{pr}} \begin{pmatrix} 1 \\ -ise^{i\varphi} \end{pmatrix}. \tag{2}$$

Here φ is the angle between the electron momentum $\mathbf{p}$ and x axis, so $e^{i\varphi}=p_x+ip_y/p$; $s=\pm 1$ denotes the branch index. The energy spectrum of the Hamiltonian (1) corresponding to two branches has the form

$$\varepsilon_{\pm}(p) = \frac{p^2}{2m} \pm \alpha p, \tag{3}$$

where $p=\sqrt{p_x^2+p_y^2}$. Using the definition $\hat{v}=d\mathbf{r}/dt=i/\hbar[H,\mathbf{r}]$, one can obtain from Eq. (1) the velocity operator components,

$$\hat{v}_x = \frac{p_x}{m} - \alpha\sigma_y, \quad \hat{v}_y = \frac{p_y}{m} + \alpha\sigma_x. \tag{4}$$

To analyze the time evolution of electron in the initial states, we use the Green's function of the nonstationary equation, which is a nondiagonal 2×2 matrix,

$$G_{ik} = \begin{pmatrix} G_{11} & G_{12} \\ G_{21} & G_{22} \end{pmatrix}. \tag{5}$$

Here $i,k=1,2$ are matrix indexes and matrix elements can be written as integrals,

$$G_{ik}(\mathbf{r},\mathbf{r}',t) = \sum_s \int d\mathbf{p}\,\phi_{\mathbf{p}s,i}(\mathbf{r},t)\phi^*_{\mathbf{p}s,k}(\mathbf{r}',0). \tag{6}$$

In this section, we examine in detail the dynamics of the quasi-1D wave packet in 2D system with spin orbit coupling. This problem allows the analytical solution. Let at the initial time $t=0$ wave function to be a plane wave with wave number p_{0x} modulated by a Gaussian profile and spin polarized along the z direction,

$$\Psi(\mathbf{r},0) = \Psi(x,0) = C\exp\left(-\frac{x^2}{2d^2} + \frac{ip_{0x}x}{\hbar}\right)\begin{pmatrix}1\\0\end{pmatrix} = f(x)\begin{pmatrix}1\\0\end{pmatrix}, \tag{7}$$

where coefficient C is equal to $(1/dL_y\sqrt{\pi})^{1/2}$ and L_y is the size of the system in the y direction. The variance of the position operator $\langle(\Delta x)^2\rangle$ in this case is equal to $d^2/2$ and the variance $\langle(\Delta y)^2\rangle$ exceeds this value. The variance of the momentum operator p_x is $\langle(\Delta p_x)^2\rangle=\hbar^2/2d^2$ and the average $\hat{\mathbf{p}}$ is equal to p_{0x}. One may consider the initial wave function as the limiting case of a 2D packet with the width along y direction, which is much greater than along x, i.e., $L_y \gg d$.

The electron wave function in any arbitrary moment of time can be found with the help of the Green's function,

$$\begin{pmatrix}\Psi_1(x,t)\\ \Psi_2(x,t)\end{pmatrix} = \int dx'dy' \begin{pmatrix} G_{11}f(x') \\ G_{21}f(x')\end{pmatrix}, \tag{8}$$

where matrix elements G_{11} and G_{21} of the matrix (5) are determined by Eqs. (2), (3), and (6),

$$G_{11}(\mathbf{r},\mathbf{r}',t) = \frac{1}{(2\pi\hbar)^2}\int \exp\left[-\frac{ip^2t}{2m\hbar} + \frac{i\mathbf{p}(\mathbf{r}-\mathbf{r}')}{\hbar}\right] \times\cos\left(\frac{\alpha pt}{\hbar}\right)d\mathbf{p}, \tag{9}$$

$$G_{21}(\mathbf{r},\mathbf{r}',t)=\frac{1}{(2\pi\hbar)^2}\int \exp\left[-\frac{ip^2t}{2m\hbar}+\frac{i\mathbf{p}(\mathbf{r}-\mathbf{r}')}{\hbar}\right]\times\sin\left(\frac{\alpha pt}{\hbar}\right)\frac{p_x+ip_y}{p}d\mathbf{p}. \quad (10)$$

By using the formula

$$e^{iq\cos\psi}=J_0(q)+2\sum_{n=1}(-1)^nJ_{2n}(q)\cos(2n\psi)+2i\sum_{n=1}(-1)^{n+1}J_{2n-1}(q)\sin[(2n-1)\psi] \quad (11)$$

and by integrating over the angle variable in Eqs. (9) and (10), we finally have

$$G_{11}=\frac{1}{2\pi\hbar^2}\int_0^\infty \exp\left[-i\frac{p^2t}{2m\hbar}J_0\left(\frac{p|\mathbf{r}-\mathbf{r}'|}{\hbar}\right)\cos\left(\frac{\alpha pt}{\hbar}\right)\right]pdp, \quad (12)$$

$$G_{21}=\frac{(x-x')+i(y-y')}{2\pi\hbar^2|\mathbf{r}-\mathbf{r}'|}\int_0^\infty \times\exp\left[-i\frac{p^2t}{2m\hbar}J_1\left(\frac{p|\mathbf{r}-\mathbf{r}'|}{\hbar}\right)\sin\left(\frac{\alpha pt}{\hbar}\right)\right]pdp, \quad (13)$$

where J_0 and J_1 are Bessel functions. Substituting Eqs. (12), (13), and (7) into Eq. (8) and integrating over x' and y', we find the analytical expression for the spinor components $\psi_{1,2}(x,t)$. It should be noted that two electron bands with chirality "plus" and "minus" give different contribution to the electron wave functions. The calculation of the expressions for $\Psi_{1,2}$ leads to the following electron probability densities $|\Psi_1|^2$ and $|\Psi_2|^2$ at any arbitrary moment of the time,

$$|\Psi_1|^2=\frac{C^2}{\sqrt{1+\gamma^2t^2}}\left\{\exp\left[-\frac{(x+(\alpha-\hbar k_0/m)t)^2}{d^2(1+\gamma^2t^2)}\right]+\exp\left[-\frac{(x-(\alpha+\hbar k_0/m)t)^2}{d^2(1+\gamma^2t^2)}\right]+2\exp\left[-\frac{(x+(\alpha-\hbar k_0/m)t)^2+(x-(\alpha+\hbar k_0/m)t)^2}{2d^2(1+\gamma^2t^2)}\right]\times\cos\left[\frac{2(k_0d^2+\gamma tx)\alpha t}{d^2(1+\gamma^2t^2)}\right]\right\}, \quad (14a)$$

$$|\Psi_2|^2=\frac{C^2}{\sqrt{1+\gamma^2t^2}}\left\{\exp\left[-\frac{(x+(\alpha-\hbar k_0/m)t)^2}{d^2(1+\gamma^2t^2)}\right]+\exp\left[-\frac{(x-(\alpha+\hbar k_0/m)t)^2}{d^2(1+\gamma^2t^2)}\right]-2\exp\left[-\frac{(x+(\alpha-\hbar k_0/m)t)^2+(x-(\alpha+\hbar k_0/m)t)^2}{2d^2(1+\gamma^2t^2)}\right]\times\cos\left[\frac{2(k_0d^2+\gamma tx)\alpha t}{d^2(1+\gamma^2t^2)}\right]\right\}, \quad (14b)$$

where $\gamma=\hbar/d^2m$ is the inverse broadening time $p_{0x}=\hbar k_0$.

As follows from Eqs. (14a) and (14b), the shape of the function $\rho(x,t)$ essentially depends on the parameter $\eta=\frac{m^2\alpha^2d^2}{\hbar^2}$. In the wide packet case, when the momentum variance is much more $(m\alpha)^2$ and the inequality $\eta\ll 1$ takes place, the evolution looks like that in the absence of Rashba term. Otherwise when $\eta\gg 1$, the initial wave packet splits into two parts, which propagate with different group velocity, so the distance between these two parts increases linearly in time. These two parts correspond to the first and second terms in square brackets in Eqs. (14a) and (14b). The third terms in Eqs. (14a) and (14b) describe the oscillation of the components of electron density $|\Psi_1|^2$ and $|\Psi_2|^2$ in the region of the overlapping of two split parts of the packet. It is clear that these oscillations originate from the interference between the states of different spectrum branches. When two parts of the packet move away from each other, the amplitude of the oscillations decreases. The period of these oscillations along the x direction depends on the initial width of the packet d and equals to $\Delta x=\pi d^2(1+\gamma^2t^2)/\alpha\gamma t^2$. So, if inequality $\gamma t\ll 1$ takes place, the period of oscillation decreases with time and equals to $\Delta x=\pi md^4/\alpha\hbar t^2$ and, when $\gamma t\gg 1$, the oscillation period does not depend on the time $\Delta x=\pi\hbar/m\alpha$.

To illustrate the evolution of the electron probability density $\rho(x,y)=|\Psi_1|^2+|\Psi_2|^2$, we plot this function using Eqs. (14a) and (14b) in Fig. 1(a) for the moments of the time $t=0$, $t=1,5$, and $t=7$ (in the units of $\tau_0=\gamma^{-1}$). The calculations were made for the parameters GaAs/InGaAs electron system $m=0.05m_0$ and $\alpha=3.6\times10^6$ cm s^{-1} and the packet parameters $d=10^{-5}$ cm and $k_0=2.5\times10^5$ cm^{-1}. Here one can clearly see that initial Gaussian wave packet [Eq. (7)] splits up at $t>0$ into two parts, propagating along the x direction. The width of each part of the packet increases in time as for the case of the free particle.

To analyze spin dynamics, one can consider the time evolution of the spin density,

$$s_i(x,y,t)=\frac{\hbar}{2}(\Psi_1^*,\Psi_2^*)\hat{\sigma}_i\begin{pmatrix}\Psi_1\\ \Psi_2\end{pmatrix}. \quad (15)$$

Using Eqs. (14a) and (14b) we immediately find the expression for spin density $s_z=\frac{\hbar}{2}(|\Psi_1(\mathbf{r},t)|^2-|\Psi_2(\mathbf{r},t)|^2)$, which demonstrates the oscillatory behavior as a function of x [see Fig. 1(b)]. The period of oscillation here is the same as for the functions $|\Psi_{1,2}(x,t)|$. For the spin density $s_y(x,t)$, the following result can be obtained:

$$s_y(x,t)=\frac{\hbar}{\sqrt{\pi}L_yd\sqrt{1+\gamma^2t^2}}\left\{\exp\left[-\frac{(x-(\hbar k_0/m-\alpha)t)^2}{d^2(1+\gamma^2t^2)}\right]-\exp\left[-\frac{(x-(\hbar k_0/m+\alpha)t)^2}{d^2(1+\gamma^2t^2)}\right]\right\}. \quad (16)$$

According to this equation both parts of the initial wave packet, moving along the x direction with different velocities, are characterized by the opposite spin orientation (at the same time the average spin component $\bar{S}_y=\int s_y(x,t)d\mathbf{r}$ is equal to zero).

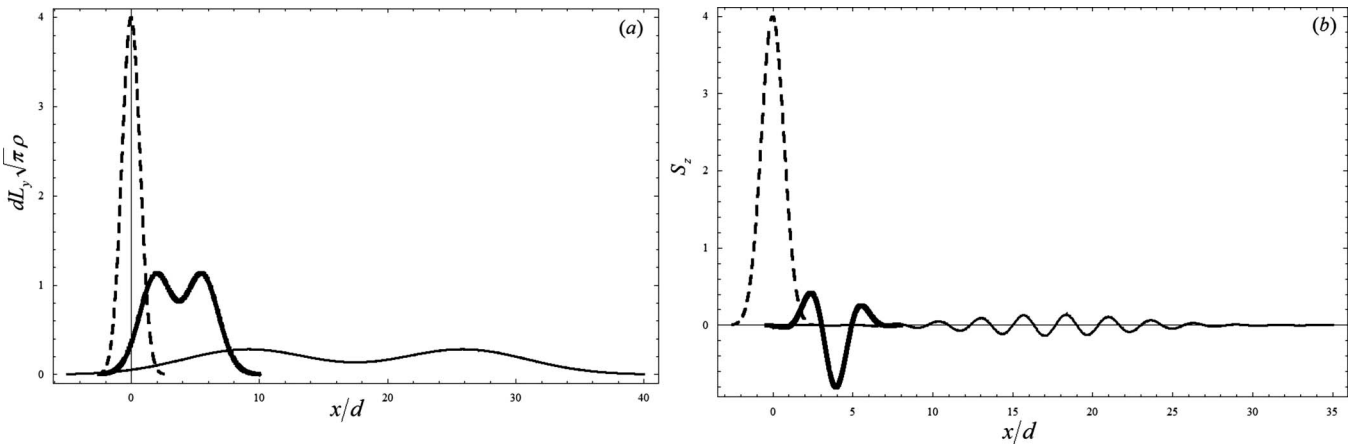

FIG. 1. (a) The electron probability density $\rho(x,t)=|\Psi_1|^2+|\Psi_2|^2$ and (b) spin density s_z. The dashed, thick, and thin lines correspond to different moments of the time, namely $t_1=0$, $t_2=1,5$, and $t_3=7$(in the units $\tau_0=\gamma^{-1}$).

Note that the components of wave function depend only on coordinate x that leads to $\bar{p}_y=p_y=0$, however, the velocity $\bar{v}_y(t)\neq 0$. Really, by using the definition in Eq. (4), it is not difficult to obtain

$$\bar{v}_x(t)=\frac{\hbar k_0}{m},\quad \bar{v}_y(t)=-\alpha\sin(2k_0\alpha t)\exp\left[-\left(\frac{\alpha t}{d}\right)^2\right]. \tag{17}$$

As follows from these equations, the average $\bar{v}_y$ velocity performs the oscillations in the transverse direction (*Zitterbewegung* or jittering) with the frequency $2k_0\alpha$ and the damping time is determined by the parameter d/α. It is not difficult to show that the space form of the packet depends on the initial spin orientation. If at the moment $t=0$ the spin is aligned parallel to the y axis, the wave functions at $t>0$ can be written as

$$\Psi(x,t)=\psi_G(x+\alpha t,t)\phi_{S_y=\hbar/2},$$

where $\phi_{S_y=\hbar/2}$ is the eigenfuction of the $\hat{\sigma}_y$ operator and ψ_G describes the evolution of a spinless particle. So, in this case, there is no packet splitting.

III. EVOLUTION OF TWO-DIMENSIONAL PACKETS AT THE PRESENCE OF SPIN ORBIT COUPLING

We consider now the evolution of 2D wave packet in the presence of spin orbit coupling. Let us consider the following form of the Gaussian packet at the initial moment $t=0$:

$$\Psi(\mathbf{r},0)=C\exp\left(-\frac{r^2}{2d^2}+\frac{ip_{0x}x}{\hbar}\right)\begin{pmatrix}1\\0\end{pmatrix}=f(\mathbf{r})\begin{pmatrix}1\\0\end{pmatrix}, \tag{18}$$

where $p_{0x}=\hbar k_0$ is the average momentum and $C=1/\sqrt{\pi}d$. Then, using a Green's function method, we arrive (after some algebra) at the following equations for the components of spinor (in the momentum space):

$$C_1(\mathbf{p},t)=\frac{d}{\sqrt{\pi}\hbar}\cos\left(\frac{\alpha pt}{\hbar}\right)\times\exp\left(-\frac{ip^2t}{2m\hbar}-\frac{p^2d^2}{2\hbar^2}-\frac{k_0^2d^2}{2}+\frac{p_xk_0d^2}{\hbar}\right), \tag{19a}$$

$$C_2(\mathbf{p},t)=-\frac{d}{\sqrt{\pi}\hbar}\frac{p_x+ip_y}{p}\sin\left(\frac{\alpha pt}{\hbar}\right)\times\exp\left(-\frac{ip^2t}{2m\hbar}-\frac{p^2d^2}{2\hbar^2}-\frac{k_0^2d^2}{2}+\frac{p_xk_0d^2}{\hbar}\right). \tag{19b}$$

After that $\Psi_{1,2}(\mathbf{r},t)$ can be obtained directly by 2D Fourier transform of $C_{1,2}(\mathbf{r},t)$,

$$\Psi_1(\mathbf{r},t)=\frac{d}{\sqrt{\pi}}\exp\left(-\frac{k_0^2d^2}{2}\right)\int_0^\infty\exp\left(-i\frac{q^2\hbar t}{2m}-\frac{q^2d^2}{2}\right)\times J_0(q\sqrt{r^2-k_0^2d^4-2ik_0d^2x})\cos(\alpha qt)qdq, \tag{20a}$$

$$\Psi_2(\mathbf{r},t)=-\frac{id}{\sqrt{\pi}}\frac{x+iy-ik_0d^2}{\sqrt{r^2-k_0^2d^4-2ik_0d^2x}}\times\exp\left(-\frac{k_0^2d^2}{2}\right)\int_0^\infty\exp\left(-i\frac{q^2\hbar t}{2m}-\frac{q^2d^2}{2}\right)\times J_1(q\sqrt{r^2-k_0^2d^4-2ik_0d^2x})\sin(\alpha qt)qdq, \tag{20b}$$

where J_0 and J_1 are the Bessel functions of the zeroth and the first orders. These expressions become simpler if the average momentum of a wave packet is equal to zero, i.e., $p_{0x}=0$. In this case,

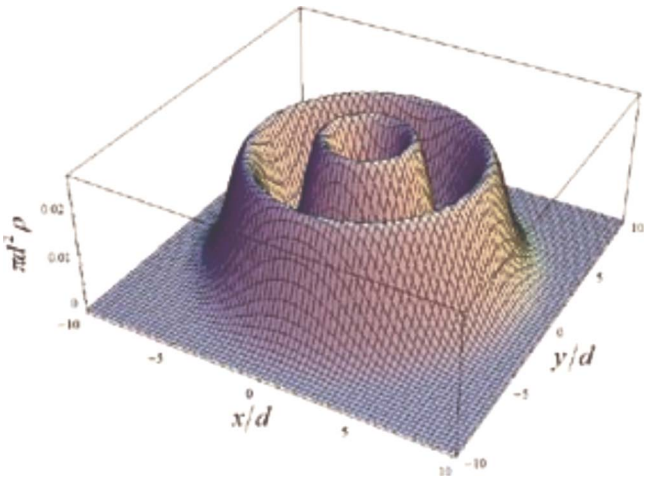

FIG. 2. (Color online) The electron probability density $\rho(x,t)=|\Psi_1|^2+|\Psi_2|^2$ for the initial-state Gaussian packet Eq. (18) with $p_{0x}=0$ at the time $t=5$ (in the units d/α).

$$\Psi_1 = \frac{d}{\sqrt{\pi}}\int_0^\infty qJ_0(qr)\cos(\alpha qt)\exp\left(-i\frac{q^2\hbar t}{2m}-\frac{q^2d^2}{2}\right)dq, \tag{21a}$$

$$\Psi_2 = \frac{d}{\sqrt{\pi}}\frac{y-ix}{r}\int_0^\infty qJ_1(qr)\sin(\alpha qt)\exp\left(-i\frac{q^2\hbar t}{2m}-\frac{q^2d^2}{2}\right)dq. \tag{21b}$$

As in the case of a 1D packet, the shape of the full electron density $\rho(x,t)=|\Psi_1|^2+|\Psi_2|^2$ at $t>0$ depends on the parameter $\eta=\frac{m^2\alpha^2d^2}{\hbar^2}$. In Fig. 2, we show the electron density $\rho(x,t)$ for the case $p_{0x}=0$ at the time $t=5$ (in the units of $\frac{d}{\alpha}$) and $\eta=2,7$. As one can see, the spin orbit coupling qualitatively changes the character of the wave packet evolution, so that during the time, the initial Gaussian packet turns into two axially symmetric parts. As follows from our analytical and numerical calculations, the outer part propagates with group velocity, which is greater than α, and the inner part moves with group velocity lower than α. If $\eta\ll 1$, i.e., the packet is narrow enough, its evolution remained the standard broadening of the Gaussian packet of free particle.

In Fig. 3(a) it is shown that the packet evolution for the case $\bar{p}_{0x}=\hbar k_0\neq 0$. It is clear that in this case, the cylindrical symmetry is absent and two maximums of the electron density spread along the x direction with unequal velocities. Each one of these two parts is spin polarized. Figure 3(b) illustrates the distribution of the spin polarization $s_y(x,y,t)$ for the initial state, which is polarized along z axis [Eq. (18)]. It is a smooth function, which has a different sign, in the regions for two maximums of the electron density.

When $\bar{p}_x\neq 0$ the motion of the wave packet centers along x, accompanied by the oscillation of the packet center in a perpendicular direction or *Zitterbewegung*. Below we consider the effect of damping of *Zitterbewegung* oscillation for 2D packet, which was not predicted in Ref. 10.

Using Eqs. (20a) and (20b) we calculate the average value of the operator $\hat{y}=i\hbar\frac{\partial}{\partial p_y}$ and obtain (for $t>0$) the result

$$\bar{y}(t) = -\frac{2d^2}{\hbar}\exp[-(k_0d)^2]\int_0^\infty \sin^2\left(\frac{\alpha pt}{\hbar}\right) \times\exp\left(-\frac{p^2d^2}{\hbar^2}\right)I_1\left(\frac{2pk_0d^2}{\hbar}\right)dp. \tag{22}$$

It is not difficult to show that this result for $\bar{y}(t)$ coincides with the expression for $-\bar{x}(t)$ in Ref. 5. In order to demonstrate this, one needs to make a summation in Eq. (8) from Ref. 5 using the expansion for modified Bessel function,[16]

$$I_1(z)=\sum_{n=0}^{\infty}\frac{(z/2)^{2n+1}}{n!\,(n+1)!}.$$

In the case when wave packet is wide enough and the inequality $a=dk_0\gg 1$ takes place, one can obtain a simple

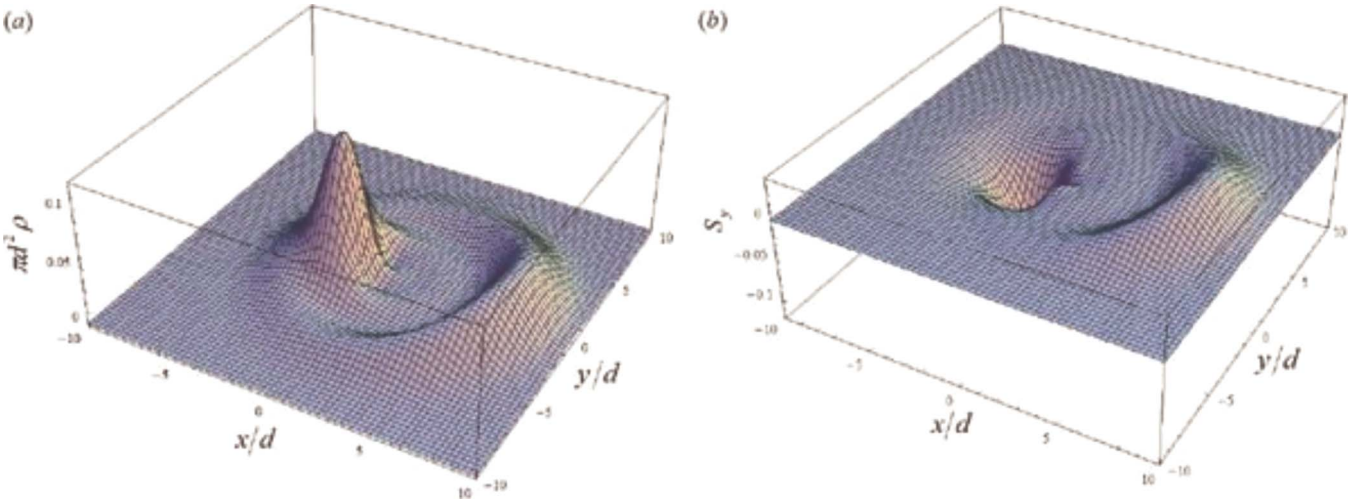

FIG. 3. (Color online) Electron density $\rho(x,t)=|\Psi_1|^2+|\Psi_2|^2$ (a) for $k_0d=2$ at the moment $t=5$ (in units d/α) and spin density $s_z(x,y,t)$ (b) at the moment $t=1,5$ (in units d/α).

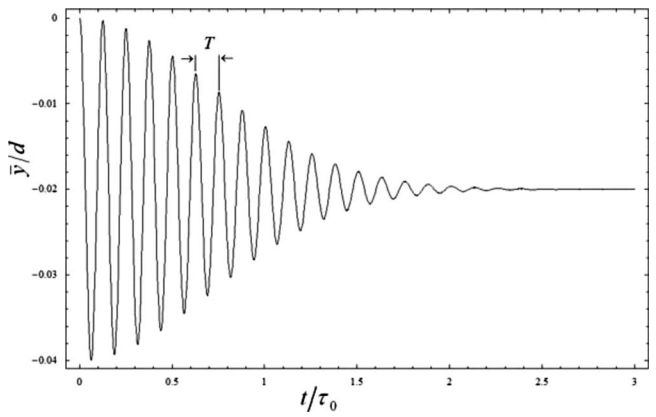

FIG. 4. The average coordinate of $\bar{y}(t)$ versus time for the packet with $k_0 d=25$.

asymptotic formula for $\bar{y}(t)$. To show this, we represent Eq. (22) as a sum of two terms,

$$\bar{y}(t) = -d\exp(-a^2)\left[\int_0^\infty \exp(-u^2) I_1(2au)du - \int_0^\infty \cos\left(\frac{2\alpha t u}{d}\right)\exp(-u^2) I_1(2au)du\right] = -d\exp(-a^2)\left\{\frac{1}{2a}[\exp(a^2)-1]-Z\right\}, \quad (23)$$

where we denote $\frac{pd}{\hbar}=u$; $Z=\mathrm{Re}[\int_0^\infty \exp(-u^2+i\frac{2\alpha t u}{d}) I_1(2au)du]$. To evaluate Z, we replace the modified Bessel function $I_1(2dk_0 u)$ by its asymptotic formula $I_1(x)=e^x/\sqrt{2\pi x}$, which is valid for the case $k_0 d \gg 1$. After that, the integral with respect to u can be evaluated using the stationary phase method that leads to the simple result,

$$Z = \frac{1}{2kd}\exp\left(a^2 - \frac{\alpha^2 t^2}{d^2}\right)\cos(2\alpha k_0 t).$$

Substituting this expression into Eq. (23), we finally have

$$\bar{y}(t) = -\frac{1}{2k_0}\left[1-\exp\left(-\frac{\alpha^2 t^2}{d^2}\right)\cos(2\alpha k_0 t)\right]. \quad (24)$$

The last result demonstrates clearly that $\bar{y}(t)$ experiences the damped oscillations with the frequency $2\alpha k_0$ decaying for the time $\frac{d}{\alpha}$. In the real 2D structures, the frequency of the *Zitterbewegung* has the order of $10^{11}-10^{12}$ s^{-1} for $k_0 \approx 10^{-5}-10^{-6}$ cm. The amplitude of the *Zitterbewegung* is proportional to the electron wavelength in x. In Fig. 4 we plot the function $\bar{y}(t)$ determined by Eq. (22), which demonstrates [in accordance with Eq. (24)] the effect of *Zitterbewegung* damping. When $t \gg \frac{d}{\alpha}$ the oscillations stop and the center of the wave packet shifts in the direction perpendicular to the group velocity at the value of $1/2k_0$. Since the packet moves with constant velocity, the time oscillations of $\bar{y}(t)$ can be easily converted to the oscillation of the wave packet center in real x,y space.

IV. CYCLOTRON DYNAMICS OF 2D WAVE PACKET IN A PERPENDICULAR MAGNETIC FIELD

In this section we examine the cyclotron dynamics of electron wave packet rotating in a magnetic field $\mathbf{B}(0,0,B)$, which is perpendicular to the plane of 2D electron gas. In this case, the one-electron Hamiltonian including the Rashba term reads

$$H = \frac{(\hat{\mathbf{p}} + e\mathbf{A}/c)^2}{2m} + \alpha[\hat{\sigma}_y(\hat{p}_x + eA_y/c) - \hat{\sigma}_x \hat{p}_y] + g\mu_B \sigma_z. \quad (25)$$

Here e is the electron charge, m is the effective mass, $\hat{p}_{x,y}$ are the momentum operator components, α is the parameter of Rashba coupling, g is the Zeeman factor, and μ_B is the Bohr magneton. Bellow, we use the Landau gauge for the vector potential $\mathbf{A}=(-By,0,0)$. Then the eigenvalues and the eigenfunctions of the Hamiltonian (25), indicating the quantum numbers n, k_x, and $s=\pm 1$, and corresponding to two branches of levels can be evaluated analytically (see, e.g., Ref. 17)

$$E_n^{\pm} = \hbar\omega_c n \pm \left(E_0^2 + \frac{2n\alpha^2\hbar^2}{\ell_B^2}\right)^{1/2}, \quad (26)$$

where $E_0^+ = \frac{\hbar\omega_c}{2} - g\mu_B B$ is the zero Landau level, $n=1,2,3,\ldots$, $\omega_c = \frac{eB}{mc}$ is the cyclotron frequency, and $\ell_B = \sqrt{\frac{\hbar}{m\omega_c}}$ is the magnetic length. The eigenspinors are

$$\psi^+_{n,k_x}(\mathbf{r}) = \frac{e^{ik_x x}}{\sqrt{2\pi A_n}}\begin{bmatrix} -iD_n\phi_{n-1}(y-y_c) \\ \phi_n(y-y_c)\end{bmatrix},$$

$$\psi^-_{n,k_x} = \frac{e^{ik_x x}}{\sqrt{2\pi A_n}}\begin{bmatrix} \phi_{n-1}(y-y_c) \\ -iD_n\phi_n(y-y_c)\end{bmatrix}, \quad (27)$$

$$\psi^+_0 = \frac{e^{ik_x x}}{\sqrt{2\pi}}\begin{bmatrix} 0 \\ \phi_0(y-y_c)\end{bmatrix}.$$

Here coefficients D_n are given by $D_n = \sqrt{2n}\alpha\hbar/\ell_B/E_0 + \sqrt{E_0^2 + 2n\alpha^2\hbar^2/\ell_B^2}$, $A_n = 1 + D_n^2$, $\phi_m(y-y_c)$ are linear oscillator wave functions, and $y_c = \ell_B^2 k_x$ is the center of oscillator. It should be noted that for enough weak magnetic field, the dependence of energy E_n^- on quantum number n ($n \gg 1$) resembles the behavior of the function $\varepsilon_-(p)$ [Eq. (3)]. Namely, for small n the values of energy E_n^+ are negative, decreasing with n, as for the hole states.

Using Eqs. (26) and (27) we can obtain components of the matrix Green's function, which permits us to find the time evolution of the initial state. The usual definition,

$$G_{ij}(\mathbf{r},\mathbf{r}',t) = \sum_{s=\pm}\int dk_x \sum_{n=0}^{\infty} \psi^s_{n,k_x,i}(\mathbf{r},t)\psi^{*s}_{n,k_x,j}(\mathbf{r},0) \quad (28)$$

yields

$$G_{11}(\mathbf{r},\mathbf{r}',t) = \frac{1}{2\pi}\int_{-\infty}^{+\infty} dk_x e^{ik_x(x-x')}\sum_{n=0} f_{n+1}(t)\phi_n(y-y_c) \times \phi_n(y'-y_c), \quad (29a)$$

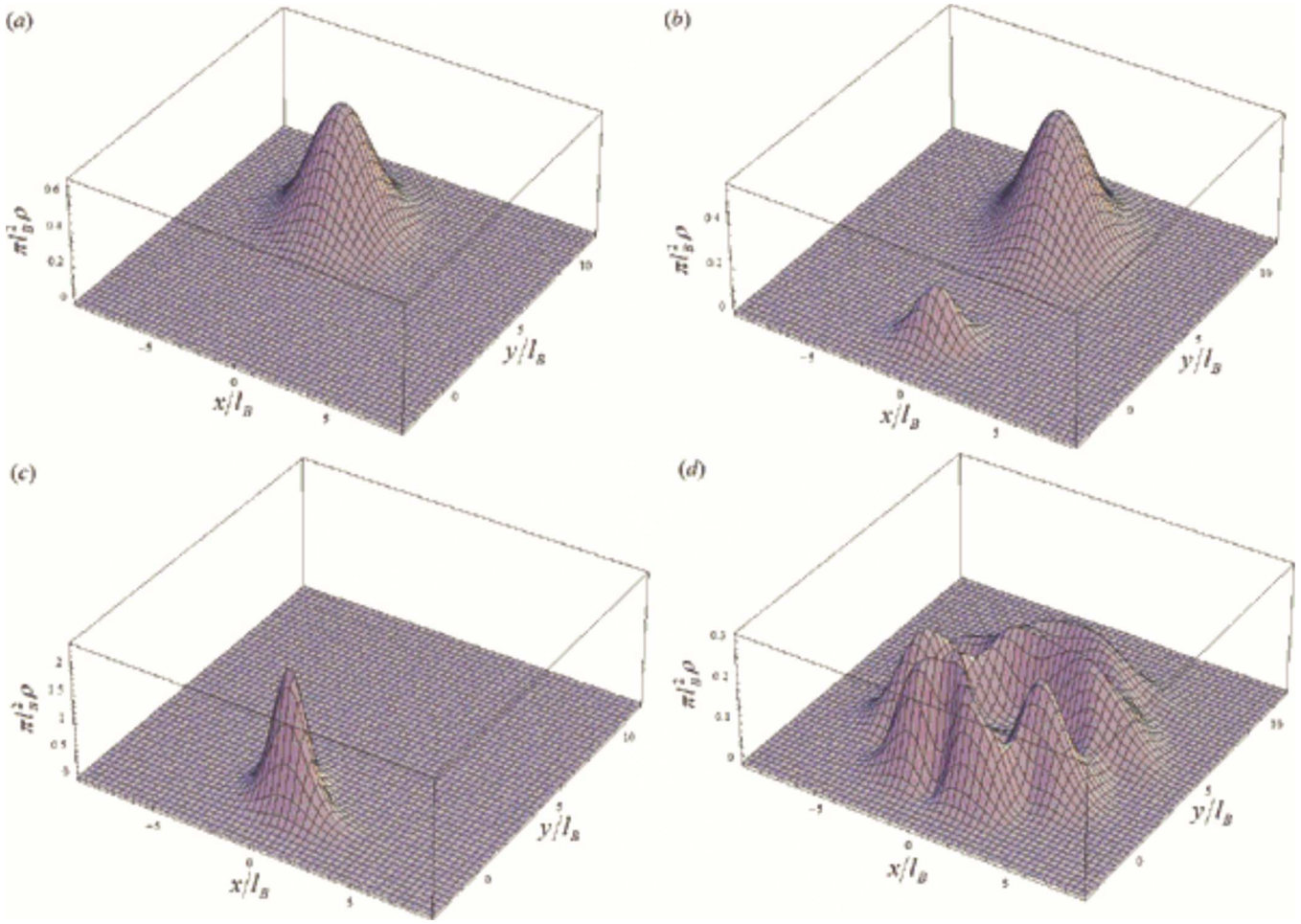

FIG. 5. (Color online) Evolution of coherent wave packet [Eq. (31)] in a perpendicular magnetic field: (a) the initial electron density Eq. (31), (b) two split packets at time $t_0 \approx 45\frac{2\pi}{\omega_c}$, (c) restored packets at time $2t_0 \approx 90\frac{2\pi}{\omega_c}$, and (d) randomized electron density for large time.

$$G_{21}(\mathbf{r},\mathbf{r}',t) = \frac{1}{2\pi}\int_{-\infty}^{+\infty} dk_x e^{ik_x(x-x')} \sum_{n=0} g_{n+1}(t)\phi_{n+1} \times (y-y_c)\phi_n(y'-y_c), \tag{29b}$$

where the time-dependent coefficients $f_n(t)$ and $g_n(t)$ are given by

$$f_n(t) = e^{-i\omega_c nt}\left[\cos\,\delta_n t - i\left(1-\frac{2}{A_n}\right)\sin\,\delta_n t\right], \tag{30a}$$

$$g_n(t) = e^{-i\omega_c nt}\frac{2D_n}{A_n}\sin\,\delta_n t, \tag{30b}$$

and $\delta_n = \frac{1}{\hbar}\sqrt{E_0^2 + \frac{2n\alpha^2\hbar^2}{\ell_B^2}}$.

Let the initial state coincide with the wave function of the coherent state in a magnetic field

$$\Psi(\mathbf{r},0) = \frac{1}{\sqrt{\pi}\ell_B^2}\exp\left(-\frac{r^2}{2\ell_B^2} + \frac{ip_{0x}x}{\hbar}\right)\begin{pmatrix}1\\0\end{pmatrix}. \tag{31}$$

Such choice of wave function $\Psi(\mathbf{r},0)$ is motivated by the following: as it is well known, in the absence of spin orbit coupling the dynamics of coherent states in a magnetic field looks like the dynamics of a classical particle. To analyze the time evolution in our case, one needs to calculate the wave function at $t>0$. Straightforward algebra, by using Eqs. (29a), (29b), and (31), leads to the final expressions

$$\psi_1(\mathbf{r},t) = \frac{1}{\sqrt{2}\pi\ell_B}\sum_{n=0}\frac{f_{n+1}(t)}{2^n n!}\int_{-\infty}^{+\infty} du e^{\varphi(x,y,u)}(-u)^n H_n\left(\frac{y}{\ell_B}-u\right), \tag{32a}$$

$$\psi_2(\mathbf{r},t) = \frac{1}{2\pi\ell_B}\sum_{n=0}\frac{g_{n+1}(t)}{2^n n!\sqrt{n+1}}\int_{-\infty}^{+\infty} du e^{\varphi(x,y,u)}(-u)^n \times H_{n+1}\left(\frac{y}{\ell_B}-u\right), \tag{32b}$$

where $\varphi(x,y,u) = iu\frac{x}{\ell_B} - \frac{(p_{0x}\ell_B/\hbar-u)^2}{2} - \frac{u^2}{4} - \frac{(y/\ell_B-u)^2}{2}$.

The electron density obtained by numerical evaluations of the integrals [Eqs. (32a) and (32b)] is represented in Fig. 5 for relatively weak spin orbit coupling and strong magnetic field. The calculations were made for the material parameters of two-dimensional GaAs heterostructure $m=0.067m_0$, $\alpha = 3.6\times10^6$ cm s^{-1}, $g=-0.44$, $B=1T$, and $k_{0x}=p_{0x}/\hbar=1.5\times10^6$ cm^{-1}. It is not difficult to verify that the series in Eqs.

(32a) and (32b) converges very rapidly as n increases. So for our parameters, it suffices to take $n_{\max}=25$ to calculate the components $\psi_1(\mathbf{r},t)$ and $\psi_2(\mathbf{r},t)$. At $t>0$ the initial wave packet [Fig. 5(a)] splits in two parts [Fig. 5(b)], which "rotate" with different incommensurable cyclotron frequencies. In accordance with Eqs. (26), these frequencies can be determined by the expression,

$$\omega_c^{\pm} = \frac{E_{n+1}^{\pm} - E_n^{\pm}}{\hbar} = \omega_c \pm \sqrt{E_0^2 + 2(n+1)\frac{\alpha^2\hbar^2}{\ell_B^2}} \mp \sqrt{E_0^2 + 2n\frac{\alpha^2\hbar^2}{\ell_B^2}}. \quad (33)$$

The effective n in this equation is connected with cyclotron radius via relation $R_c(t)=\frac{p_{0x}}{m\omega_c}=\sqrt{2n}\ell_B$. Believing that $\varsigma = \frac{2n\alpha^2\hbar^2}{\ell_B^2 E_0^2} \ll 1$, i.e., in the case of a weak spin orbit coupling or strong magnetic field, one can obtain [from Eq. (33)] the approximate expression for the difference between cyclotron frequencies

$$\omega_c^+ - \omega_c^- = 2\frac{\alpha^2 m}{E_0}\omega_c. \quad (34)$$

Figure 5(b) demonstrates, for the case $\varsigma \ll 1$, the distribution of electron density at the moment when two parts are located at opposite points of the cyclotron orbit. The correspondent time can be determined from the relation $(\omega_c^+ - \omega_c^-)t_0=\pi$ and, hence, for the GaAs structure we will have $t_0=\frac{\pi}{\omega_c^+ - \omega_c^-} = \frac{\pi}{\omega_c}\frac{E_0}{2\alpha^2 m}=45\frac{2\pi}{\omega_c}$.

After some cyclotron periods, two split packets merge again, which are demonstrated in Fig. 5(c). With time due to the effect of the broadening, electron probability distributes randomly around cyclotron orbit, which is shown in Fig. 5(d).

In the opposite case of relatively strong spin orbit coupling or weak magnetic field when the inequality $\varsigma=\frac{2n\alpha^2\hbar^2}{\ell_B^2 E_0^2} \gg 1$ holds true, the difference between two cyclotron frequencies, as it follows from Eq. (33), equals to $\omega_c^+ - \omega_c^- = \frac{\sqrt{2}\alpha}{\sqrt{n}\ell_B}$. For the InGaAs structure with parameters $m=0.05m_0$, $\alpha=3.6\times10^6$ cm s^{-1}, $g=-10$, $B=1T$, and $k_{0x}=p_{0x}/\hbar=1.5\times10^6$ cm^{-1} we have $\varsigma=8$ and the divergence time $t_0 \approx 2.3\frac{2\pi}{\omega_c}$.

One can analyze the effects of the periodic splitting and reshaping of the wave packet in magnetic field, as well as the process of distribution around cyclotron orbit, by considering the time dependence of the cyclotron radius determined as $R(t)=\sqrt{\{\bar{x}(t)\}^2+\{\bar{y}(t)\}^2}$. To do this we represent the average value of coordinates $x_1=x$ and $x_2=y$ as

$$\bar{x}_i = \int \psi_1^*(\mathbf{r},t)x_i\psi_1(\mathbf{r},t)d\mathbf{r} + \int \psi_2^*(\mathbf{r},t)x_i\psi_2(\mathbf{r},t)d\mathbf{r}, \quad (35)$$

where ψ_1 and ψ_2 are determined by Eqs. (32a) and (32b). The lengthy calculations (see the Appendix) eventually yield the explicit expressions for the $\bar{x}(t)$ and $\bar{y}(t)$,

$$\bar{x}(t) = -\frac{\ell_B}{3}e^{-p_{0x}^2\ell_B^2/3\hbar^2}\left\{\cos\omega_c t\sum_{k=0} S_k(t)H_{2k+1}\left(i\sqrt{\frac{2}{3}}p_{0x}\ell_B/\hbar\right) + \sin\omega_c t\sum_{k=0} P_k(t)H_{2k+1}\left(i\sqrt{\frac{2}{3}}p_{0x}\ell_B/\hbar\right)\right\}, \quad (36a)$$

$$\bar{y}(t) = q\ell_B^2 + \frac{\ell_B}{3}e^{-p_{0x}^2\ell_B^2/3\hbar^2}\left\{\cos\omega_c t\sum_{k=0} P_k(t)H_{2k+1}\left(i\sqrt{\frac{2}{3}}p_{0x}\ell_B/\hbar\right) - \sin\omega_c t\sum_{k=0} S_k(t)H_{2k+1}\left(i\sqrt{\frac{2}{3}}p_{0x}\ell_B/\hbar\right)\right\}. \quad (36b)$$

As one can see, the dependence of $\bar{x}(t)$ and $\bar{y}(t)$ on the time are determined by both factors cos $\omega_c t$ and sin $\omega_c t$, as well as by functions,

$$S_k(t) = i\frac{(-1)^k}{k!}\left(\frac{1}{12}\right)^k[\xi_{k+2}\cos\delta_{k+1}t\sin\delta_{k+2}t - \xi_{k+1}\cos\delta_{k+2}t\sin\delta_{k+1}t], \quad (37a)$$

$$P_k(t) = i\frac{(-1)^k}{k!}\left(\frac{1}{12}\right)^k\left[\cos\delta_{k+1}t\cos\delta_{k+2}t + \left(\xi_{k+1}\xi_{k+2} + 4\sqrt{\frac{k+2}{k+1}}\frac{D_{k+1}D_{k+2}}{A_{k+1}A_{k+2}}\right)\sin\delta_{k+1}t\cos\delta_{k+2}t\right],$$

$$\xi_k = \frac{D_k^2-1}{D_k^2+1}, \quad (37)$$

which describe the additional time dependence due to spin precession. Note that the frequencies $\delta_k=\frac{1}{\hbar}\sqrt{E_0^2+\frac{2k\alpha^2\hbar^2}{\ell_B^2}}$ are incommensurable. As a check on this formalism, it is not difficult to show that in the absence of Rashba coupling ($\alpha=0$), as it follows from Eqs. (36a) and (36b),

$$\bar{x}(t) = p_{0x}\ell_B^2/\hbar\sin\omega_c t,\ \ \bar{y}(t) = p_{0x}\ell_B^2(1-\cos\omega_c t), \quad (38)$$

that corresponds to the classical motion of charged particle in the magnetic field with a constant radius.

The time dependence of the cyclotron radius $R(t)$ in the system with Rashba is presented in Fig. 6. It is clear that the oscillations of $R(t)$ are connected with the effects of periodic splitting and reshaping of wave packets. The radius has the minimal values at the moments when two parts of the packet are located at the opposite point of cyclotron orbit. This situation is shown in Fig. 5(b). The first minimum is labeled by the letter b in Fig. 6. One can see that the time of the first minimum approximately coincides to our estimation made above, $t_0 \approx 45T_c$. The radius is maximal at the moments of the packet reshaping, which is shown in Fig. 5(c) (two of these points are labeled by the letters a and c). Due to the effects of incommensurability of the cyclotron frequencies and the packet broadening, the amplitude of the oscillations decreases with the time. After that, the electron density distributes around cyclotron orbit, the amplitude of the oscillation ceases, and the electron-density distribution acquires the

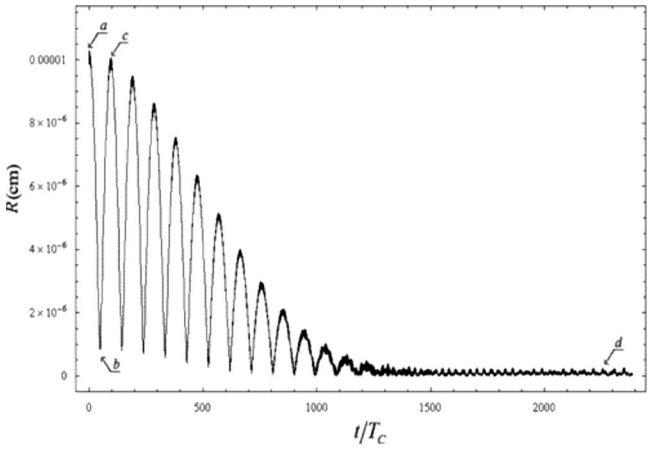

FIG. 6. Cyclotron radius plotted versus the time (for the same parameters as in Fig. 5). The distance between maximums and minimums of $R(t)$ marked by arrows is approximately equal to $80T_c$, time is measured in units of cyclotron period $T_c=\frac{2\pi}{\omega_c}$. The points a, b, c, and d correspond to the same moments of time as in Figs. 5(a)–5(d), respectively.

no-regular character [Fig. 5(d)]. Note here that the numerical simulation of the radius of electron orbit $R(t)$ was made in Ref. 15, only for small t, that corresponds to the time interval near the first maximum in Fig. 6.

We evaluate also the distribution of the electron density for the structure with relatively strong spin orbit coupling. For such systems, instead of the repeated process of the splitting and restoring of the wave packet as discussed above, the transition to the irregular distribution along the cyclotron orbit can be realized for the time of the order of one cyclotron period.

V. CONCLUSIONS

We have analyzed the evolution of 1D and 2D wave packets in 2D electron gas with linear Rashba spin orbit coupling. We showed that the electron packet dynamics differs drastically from usual quantum dynamics of electrons with parabolic energy spectrum. Depending on the initial spin polarization packet splits in two parts which propagate with different velocities and have different spin orientation. At the time when two parts of the wave packet overlap, the packet center performs oscillations in much the same way as for a relativistic particle. The direction of these oscillations is perpendicular to the packet group velocity. When the distance between split parts exceeds the initial width of the packet, these oscillations stop.

In the 2D semiconductor structures placed in a perpendicular magnetic field, the spin orbit coupling changes the cyclotron dynamics of charged particles. As in the absence of magnetic field, the initial packet splits in two parts, which rotate in a perpendicular magnetic field with different incommensurable cyclotron frequencies. As a result, after some cyclotron periods these parts join again. The corresponding time t_0 essentially depends upon the ratio of the energy of spin orbit coupling and the distance between Landau levels [Eq. (26)]: $\varsigma=\frac{2n\alpha^2\hbar^2}{\ell_B^2 E_0^2}$. Thus, for the systems with weak and relatively strong spin orbit couplings, e.g., GaAs and InGaAs heterostructures, the time t_0 equals to $45T_c$ and $2,3T_c$, respectively.

The splitting and *Zitterbewegung* of the wave packets in nanostructures with spin orbit coupling can be observed experimentally in low-dimensional structures. In particular, these effects should determine the electron dynamics and high-frequency characteristics of the field effect transistor by Datta and Das[18] and other spintronic devices. Simple estimations show that, during the time of the wave packet propagation through the ballistic transistor channel where the distance between emitter and collector is of the order of 1 μm, the distance between two split parts of the wave packet becomes comparable with its initial size. In this situation, the high-frequency characteristics of the field effect transistor should be substantially affected by the spin orbit coupling. Moreover, the atypical semiclassical dynamics of a spin orbit system placed in a magnetic field will influence the shape of the cyclotron resonance line in 2D systems with spin orbit coupling. An important feature of these experiments is that the electron transport is in the ballistic regime and, thus, the momentum relaxation time τ should be considered much more greater compared to the typical splitting time.

ACKNOWLEDGMENTS

The authors are grateful to D.V. Khomitsky for useful discussions. This work was supported by the program of the Russian Ministry of Education and Science "Development of scientific potential of high education" (Project No. 2.1.1.2363).

APPENDIX

This Appendix provides some of the details involved in obtaining the average value of the position operator given by Eqs. (36a) and (36b). According to Eq. (35),

$$\bar{y}(t)=\bar{y}_1(t)+\bar{y}_2(t). \tag{A1}$$

Consider the calculation of the first term $\bar{y}_1(t)$. Using the initial wave function [Eq. (31)], we obtain

$$\bar{y}_1(t)=\int\int\frac{d\mathbf{r}'d\mathbf{r}''}{\pi\ell_B^2}\exp\left[-\frac{r'^2+r''^2}{2\ell_B^2}+\frac{ip_{0x}(x'-x'')}{\hbar}\right]\int G_{11}(\mathbf{r},\mathbf{r}',t)yG_{11}^*(\mathbf{r},\mathbf{r}'',t)d\mathbf{r}. \tag{A2}$$

The last integral in this equation is denoted as

$$M_{11}^y=\int G_{11}(\mathbf{r},\mathbf{r}',t)yG_{11}^*(\mathbf{r},\mathbf{r}'',t)d\mathbf{r}. \tag{A3}$$

Then substituting Eq. (29a) into Eq. (A3) and using the well-known formula for a linear harmonic-oscillator function,

$$\int_{-\infty}^{+\infty} y\phi_n(y-y_c)\phi_k(y-y_c)dy$$

$$= \frac{\ell_B}{\sqrt{2}}(\sqrt{n}\delta_{k,n-1} + \sqrt{n+1}\,\delta_{k,n+1}) + y_c\delta_{n,k}, \quad \text{(A4)}$$

we will have

$$M_{11}^{y} = \frac{1}{2\pi}\int_{-\infty}^{+\infty} e^{ik_x(x-x'')}\mu(y',y'',t,y_c)dk_x. \quad \text{(A5)}$$

Here

$$\mu(y',y'',t,y_c) = \frac{\ell_B}{\sqrt{2}}\sum_{n=0}\sqrt{n}f_{n+1}(t)f_n^*(t)\phi_n(y'-y_c)\phi_{n-1}(y''-y_c)$$
$$+ \frac{\ell_B}{\sqrt{2}}\sum_{n=0}\sqrt{n+1}f_{n+1}(t)f_{n+2}^*(t)\phi_n(y'$$
$$- y_c)\phi_{n+1}(y''-y_c) + y_c\sum_{n=0}|f_{n+1}(t)|^2\phi_n(y'$$
$$- y_c)\phi_n(y-y_c), \quad \text{(A6)}$$

where the coefficients $f_n(t)$ are given by Eq. (30a). We calculate $\bar{y}_1(t)$ by substituting Eqs. (A5) and (A6) into Eq. (A2). The resulting integrals can be evaluated by using Gaussian transformation[16]

$$\frac{1}{\sqrt{\pi}}\int_{-\infty}^{+\infty} e^{-(x-y)^2}H_n(y)dy = (2x)^n, \quad \text{(A7)}$$

$$\frac{1}{\sqrt{\pi}}\int_{-\infty}^{+\infty} e^{-(x-y)^2}y^n dy = \frac{H_n(ix)}{(2i)^n}.$$

Finally, we obtain

$$\bar{y}_1(t) = \frac{\ell_B}{6}\exp\left[-\frac{(p_{0x}\ell_B)^2}{3\hbar^2}\right]\sum_{k=0}\psi_k(t)H_{2k+1}(i\sqrt{2/3}p_{0x}\ell_B/\hbar), \quad \text{(A8)}$$

where

$$\psi_k(t) = \frac{i}{k!}\left(-\frac{1}{12}\right)^k(f_{k+1}^*(t)f_{k+2}(t) + f_{k+1}(t)f_{k+2}^*(t) - 2|f_{k+1}(t)|^2). \quad \text{(A9)}$$

Performing the same kind of calculation, we have [for $\bar{y}_2(t)$]

$$\bar{y}_2(t) = \frac{\ell_B}{6}\exp\left[-\frac{(p_{0x}\ell_B)^2}{3\hbar^2}\right]\sum_{k=0}\gamma_k(t)H_{2k+1}(i\sqrt{2/3}p_{0x}\ell_B/\hbar), \quad \text{(A10)}$$

where

$$\gamma_k(t) = \frac{i}{k!}\left(-\frac{1}{12}\right)^k(g_{k+1}^*(t)g_{k+2}(t) + g_{k+1}(t)g_{k+2}^*(t) - 2|g_{k+1}|^2) \quad \text{(A11)}$$

and the coefficients $f_k(t)$ and $g_k(t)$ in Eqs. (A9) and (A11) are determined by Eqs. (30a) and (30b). The preceding expressions immediately lead to the average value $\bar{y}(t)$ given in Eq. (36b). The evaluation of $\bar{x}(t)$ can be obtained by following the procedure similar to that, which led to Eq. (36a).

*demi@phys.unn.ru

[1] J. Schliemann, Int. J. Mod. Phys. B **20**, 1015 (2006).

[2] H.-A. Engel, E. I. Rashba, and B. I. Halperin, *Handbook of Magnetism and Advanced Magnetic Materials* (Wiley, New York, in press), Vol. 5.

[3] I. Zutic, J. Fabian, and S. Das Sarma, Rev. Mod. Phys. **76**, 323 (2004).

[4] Yu. A. Bychkov and E. I. Rashba, Pis'ma Zh. Eksp. Teor. Fiz. **39**, 66 (1984) [JETP Lett. **39**, 78 (1984)].

[5] J. Schliemann, D. Loss, and R. M. Westervelt, Phys. Rev. Lett. **94**, 206801 (2005).

[6] J. Schliemann, D. Loss, and R. M. Westervelt, Phys. Rev. B **73**, 085323 (2006).

[7] Z. F. Jiang, R. D. Li, S.-C. Zhang, and W. M. Liu, Phys. Rev. B **72**, 045201 (2005).

[8] M. Khodas, A. Shekhter, and A. Finkelstein, Phys. Rev. Lett. **92**, 086602 (2004).

[9] A. Shekhter, M. Khodas, and A. M. Finkel'stein, Phys. Rev. B **71**, 125114 (2005).

[10] H. Chen, J. J. Heremans, J. A. Peters, A. O. Govorov, N. Goel, S. J. Chung, and M. B. Santos, Appl. Phys. Lett. **86**, 032113 (2005).

[11] G. Usaj and C. A. Balseiro, Phys. Rev. B **70**, 041301(R) (2004).

[12] L. P. Rokhinson, V. Larkina, Y. B. Lyanda-Geller, L. N. Pfeiffer, and K. W. West, Phys. Rev. Lett. **93**, 146601 (2004).

[13] R. Winkler, U. Zülicke, and J. Bolte, Phys. Rev. B **75**, 205314 (2007).

[14] U. Zülicke, J. Bolte, and R. Winkler, New J. Phys. **9**, 355 (2007).

[15] J. Schliemann, Phys. Rev. B **77**, 125303 (2008).

[16] I. S. Gradshteyn and I. M. Ryzhik, *Tables of Integrals, Series and Products* (Academic, New York, 1980).

[17] X. F. Wang and P. Vasilopoulos, Phys. Rev. B **67**, 085313 (2003).

[18] S. Datta and B. Das, Appl. Phys. Lett. **56**, 665 (1990).